

Electronic method for suppressing output instability of GMI sensors caused by the orientation

Dasha Zhang^{a)}, Zhongming Pan, Zhang Zhuohang,
and Wenna Zhang

*College of Mechatronics Engineering and Automation, National University of
Defense Technology, Changsha 410073, China*

a) zhangsha1024@163.com

Abstract: Magnetic sensors based on the giant magneto-impedance effect (GMI sensors) have a promising application prospect in the field of magnetic anomaly detection for their high resolution. However, they are highly sensitive to its orientation without any magnetic shielding. A method that automatically adjusts the bias magnetic field to make it always work on its initial value is proposed in order to suppress output instability of GMI sensors caused by the orientation. The analog circuit implementing the method is designed according to the principle of feedback control. The experimental results demonstrated the effectiveness of the proposed method.

Keywords: giant magneto-impedance effect, magnetic sensor, bias magnetic field, orientation, feedback control

Classification: Integrated circuits

References

- [1] B. Ginzburg, *et al.*: “Processing of magnetic scalar gradiometer signals using orthonormalized functions,” *Sens. Actuators A* **102** (2002) 67 (DOI: [10.1016/S0924-4247\(02\)00351-5](https://doi.org/10.1016/S0924-4247(02)00351-5)).
- [2] A. Sheinker, *et al.*: “Magnetic anomaly detection using high-order crossing method,” *IEEE Trans. Geosci. Remote Sens.* **50** (2012) 1095 (DOI: [10.1109/TGRS.2011.2164086](https://doi.org/10.1109/TGRS.2011.2164086)).
- [3] M. H. Phan and H. X. Peng: “Giant magnetoimpedance materials: Fundamentals and applications,” *Prog. Mater. Sci.* **53** (2008) 323 (DOI: [10.1016/j.pmatsci.2007.05.003](https://doi.org/10.1016/j.pmatsci.2007.05.003)).
- [4] B. Dufay, *et al.*: “Impact of electronic conditioning on the noise performance of a two-port network giant magnetoimpedance magnetometer,” *IEEE Sensors J.* **11** (2011) 1317 (DOI: [10.1109/JSEN.2010.2084996](https://doi.org/10.1109/JSEN.2010.2084996)).
- [5] B. Fisher, *et al.*: “High performance current sensor utilizing pulse magneto-impedance in Co-based amorphous wires,” *IEEE Trans. Magn.* **49** (2013) 89 (DOI: [10.1109/TMAG.2012.2220958](https://doi.org/10.1109/TMAG.2012.2220958)).
- [6] J. Lenz and S. Edelstein: “Magnetic sensors and their applications,” *IEEE Sensors J.* **6** (2006) 631 (DOI: [10.1109/JSEN.2006.874493](https://doi.org/10.1109/JSEN.2006.874493)).
- [7] J. Olivera, *et al.*: “Comprehensive analysis of a micro-magnetic sensor performance using amorphous microwire MI element with pulsed excitation

- current,” *Sens. Actuators A* **168** (2011) 90 (DOI: [10.1016/j.sna.2011.04.012](https://doi.org/10.1016/j.sna.2011.04.012)).
- [8] E. C. Silva, *et al.*: “Electronic approach for enhancing impedance phase sensitivity of GMI magnetic sensors,” *Electron. Lett.* **49** (2013) 396 (DOI: [10.1049/el.2012.3018](https://doi.org/10.1049/el.2012.3018)).
- [9] J. S. Liu, *et al.*: “Twin-detector sensor of Co-rich amorphous microwires to overcome GMI fluctuation induced by ambient temperature,” *IEEE Trans. Magn.* **48** (2012) 2449 (DOI: [10.1109/TMAG.2012.2192132](https://doi.org/10.1109/TMAG.2012.2192132)).
- [10] K. Mohri, *et al.*: “Sensitive micro magnetic sensor family utilizing magneto-impedance (MI) and stress-impedance (SI) effects for intelligent measurements and controls,” *Sens. Actuators A* **91** (2001) 85 (DOI: [10.1016/S0924-4247\(01\)00620-3](https://doi.org/10.1016/S0924-4247(01)00620-3)).

1 Introduction

Magnetic anomaly detection (MAD) is a widespread technique used to determine the presence and some characteristics of visually obscured ferromagnetic objects by revealing the anomalies in the uniform geomagnetic field [1, 2]. In general, the magnetic anomaly signal induced by the ferromagnetic object is rather weak for remote sensing applications. Magnetic sensors based on the giant magneto-impedance effect (GMI sensors) have great potential to be employed as magnetic anomaly detectors for their extremely high resolution [3, 4, 5]. However, as a vector sensor, the GMI sensor is highly sensitive to its orientation due to the uniform geomagnetic field in no any magnetically shielded space (NMSS) [6]. Because the magnetic anomaly signal is relatively smaller than the uniform geomagnetic field, even a slight orientation change will cause the output of the GMI sensor to rise or fall. Unfortunately, these variations in the external magnetic field induced by the orientation are often large enough to exceed the linear range of the GMI sensor and cause the GMI sensor to be unable to work normally. In order to overcome the effect of the orientation associated with the experiments, GMI sensors are always situated either in a magnetically shielded space (MSS) or in a way to keep its sensing direction perpendicular to the uniform geomagnetic field [7, 8, 9]. However, from the perspective of engineering application, it is troublesome and sometimes unpractical to always fulfill the conditions mentioned above. Therefore, an electronic method is proposed to suppress the output instability of GMI sensors caused by the orientation.

2 Proposed method

The Co-rich amorphous wire is utilized as the sensing element in the GMI sensor. At the condition of a strong skin effect, the impedance Z in an amorphous wire specimen as a function of the external magnetic field H_{ex} can be expressed as:

$$Z = \frac{a}{2\sqrt{2\rho}} R_{dc}(1 + j)\sqrt{\omega\mu(H_{ex})} \quad (1)$$

where a is the radius of the wire, R_{dc} is the DC resistance of the wire, ρ is the resistivity, ω is the angular frequency of the current flowing along the specimen, $\mu(H_{ex})$ is the circumferential maximum differential permeability and j is the imaginary unit, respectively [10]. Schematic illustration of the electronics setup

used to measure the GMI characteristics of the amorphous wire is presented in Fig. 1. A programmable current power supply provided drive current for the Helmholtz coil in order to generate external DC magnetic field. The amorphous wire specimen with a diameter of about 30 μm and a whole length of about 15 mm was connected into sensor circuit by the silver conductive paint (each fixed terminal about 2.5 mm long). The final output voltage V_{out} of the GMI sensor circuit was observed by means of the digital oscilloscope.

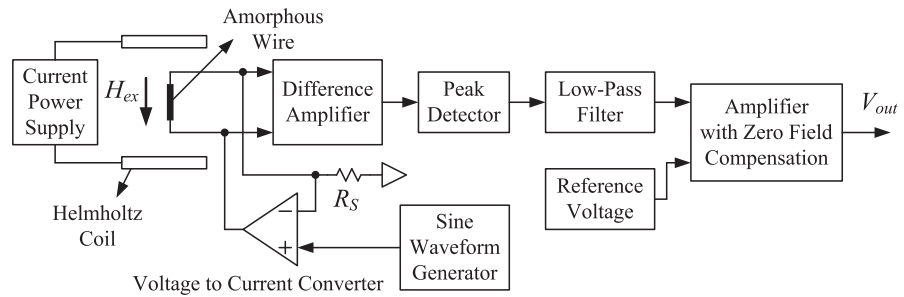


Fig. 1. Block diagram of the setup used to measure the GMI characteristics of the amorphous wire

Fig. 2 shows measured results of magnitude change of the final output voltage V_{out} when the specimen was subjected to the sinusoidal current with a frequency of 12 MHz and an amplitude of 15 mA in MSS at room temperature. Since the GMI profile exhibits an unipolar and nonlinear response at the near-zero magnetic field, an operating point is required for the GMI sensor to determine the sign of the external magnetic field and sensitivity. An initial bias magnetic field H_{b0} of about 1 Oe is used to set the operating point at P_0 .

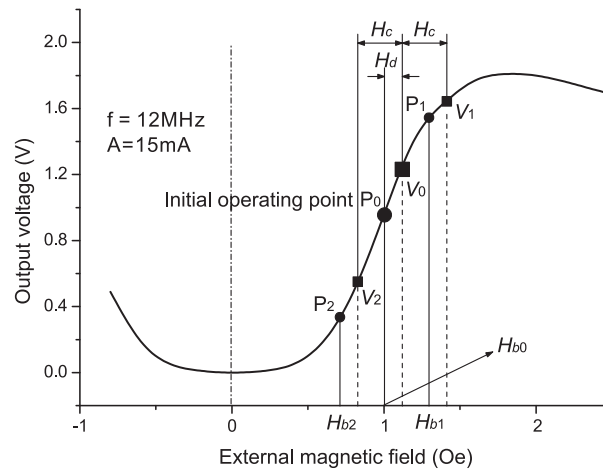


Fig. 2. GMI profile of the amorphous wire

The vector component of the uniform geomagnetic field along the axis of the specimen H_c , which is superimposed on the detected signal H_d , leads to magneto-impedance fluctuation of the specimen and consequently the final output fluctuation. When the sensing direction of the GMI sensor is adjusted perpendicular to the

uniform geomagnetic field in NMSS, the vector component H_c is equal to zero. However, the orientation change will induce variations in the vector component. As shown in Fig. 2, the final output voltage V_{out} corresponding to the same detected signal H_d varies from V_0 to V_1 or V_2 . As a function of the external magnetic field, the final output voltage V_{out} before and after the orientation change can be expressed as:

$$\begin{cases} V_0 = F(H_{b0} + H_d) \\ V_1 = F[H_{b0} + (H_d + H_c)] \\ V_2 = F[H_{b0} + (H_d - H_c)] \end{cases} \quad (2)$$

where V_0 is the final output voltage corresponding to H_d at $H_c = 0$, V_1 and V_2 are the final output voltage corresponding to H_d when H_c has the same and opposite direction with H_d , respectively.

By analyzing the behavior of the external magnetic field applying on the specimen, the vector component H_c can be considered as a disturbance signal superimposed on the initial bias magnetic field H_{b0} instead of the detected signal H_d . Thus, the equation (2) can be written as:

$$\begin{cases} V_0 = F(H_{b0} + H_d) \\ V_1 = F[(H_{b0} + H_c) + H_d] = F(H_{b1} + H_d) \\ V_2 = F[(H_{b0} - H_c) + H_d] = F(H_{b2} + H_d) \end{cases} \quad (3)$$

According to the equation (3), the bias magnetic field H_b varies from H_{b0} to H_{b1} or H_{b2} . Correspondingly, the operating point is shifted from P_0 to P_1 or P_2 , as shown in Fig. 2. As a result, the output fluctuation could be ascribed to the variation in the bias magnetic field. Therefore, it is possible to suppress the output fluctuation by automatically adjusting H_b to make it always work in its initial value.

3 Analog circuit implementing the proposed method

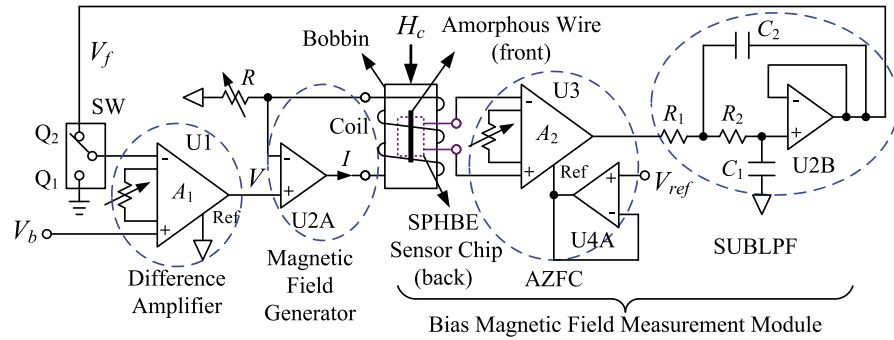
An analog circuit implementing the proposed method was developed according to the principle of feedback control. The developed circuit consists of a difference amplifier, a magnetic field generator and a bias magnetic field measurement module, as shown in Fig. 3. The constant voltage V_b is used for setting the bias magnetic field in the coil H_b . The feedback voltage V_f is compared with V_b by the difference amplifier (U1) and the subtraction voltage is amplified by the gain A_1 . The magnetic field generator using the operational amplifier (U2A) converts the input voltage V to the magnetic field H_{bi} through the bias coil and the current sampling resistor R . The bias magnetic field measurement module composed of the SPHBE magnetic sensor chip with large scale, the difference amplifier (U3) with zero field compensation (AZFC) and the second-order unity-gain Butterworth low-pass filter (SUBLPF) based on the operational amplifier (U2B) is used as the feedback loop. It detects the bias magnetic field H_b and provides feedback voltage V_f to the inverting input of the difference amplifier (U1). The instrumentation amplifier is used in both difference amplifiers (U1 and U3) in order to conveniently adjust the gain, and the operational amplifier (U4A) with low noise and high input impedance is utilized as the voltage buffer in the AZFC. The magnetic field H_{bi} , generated by the bias coil with a DC current, can be expressed as:

$$H_{bi} = \frac{N}{L} I = \frac{N}{L} \frac{1}{R} V \quad (4)$$

where N and L are the winding number and length of the bias coil, respectively. The feedback voltage V_f can be expressed as:

$$V_f = H_b S A_2 \quad (5)$$

where A_2 is the gain of the AZFC and S is the sensitivity of the SPHBE sensor chip. It is obvious that the feedback voltage V_f is proportional to the bias magnetic field H_b . Consequently, we can obtain the bias magnetic field H_b by measuring the feedback voltage V_f .



U1, U3: INA128, U2: OPA2227, U4: AD822,
 R_1 : 180k Ω , R_2 : 300k Ω , C_1 : 0.47 μ F, C_2 : 1 μ F.

Fig. 3. Structure of the developed circuit

The block diagram model of the developed circuit is shown in Fig. 4. Using Mason's rule, the bias magnetic field due to the two inputs is

$$H_b(s) = \frac{A_1 \frac{N}{RL}}{1 + A_1 \frac{N}{RL} S A_2 G(s)} V_b(s) + \frac{1}{1 + A_1 \frac{N}{RL} S A_2 G(s)} H_c(s) \quad (6)$$

where A_1 is the gain of the difference amplifier and $G(s)$ is the transfer function of the SUBLPF. $G(s)$ can be expressed as:

$$G(s) = \frac{1}{s^2 + 1.4142s + 1} \quad (7)$$

according to the equations (6) and (7), the characteristic equation of the developed circuit is written as:

$$s^2 + 1.4142s + \left(1 + A_1 \frac{N}{RL} S A_2\right) = 0 \quad (8)$$

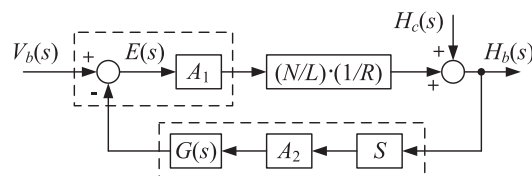


Fig. 4. Block diagram model of the developed circuit

For all coefficients in the equation (8) are positive numbers, all the roots of the characteristic equation are in the left-hand s-plane. Thus, the developed circuit is stable.

According to the block diagram model in Fig. 4, the magnetic signals with lower frequency than the SUBLPF cut-off frequency will be attenuated sharply. Therefore, the GMI sensor with the developed circuit is especially suitable for the detection of the AC and transient magnetic field signals. In addition, the weak magnetic signals with smaller intensity than the resolution of the SPHBE sensor chip, whether their frequency is high or low, can pass through the developed circuit. Owing to the higher resolution of the GMI sensor, it is possible for the GMI sensor with the developed circuit to realize the detection of the weak magnetic signals.

4 Results and discussion

According to the developed circuit, a novel GMI sensor head was designed. The specimen was fixed on one side of the printed circuit board (PCB) by the silver conductive paint and the SPHBE sensor chip was welded on the other side of the PCB by soldering tin. The bias coil was made by an enameled C_u wire wrapped around the bobbin. The winding number N , the length L , and the sensitivity S at the supply power of +2.048 V and Ground were 510 turns, 30 mm and 55.14 mV/mT, respectively.

To examine the performance of the developed circuit, a circuit without feedback was used as the control group. The SUBLPF cut-off frequency of 1 Hz, the resistor R of 200 Ω , the gain A_1 of 50 and the gain A_2 of 174 were set. The developed circuit can be configured as the circuit without feedback when the switch SW is toggled to Q_1 and the gain A_1 is set to 1. Aiming at generating the H_{b0} of 1 Oe at $H_c = 0$, the desired voltage V_b for the developed circuit and the circuit without feedback were set to 0.978 V and 0.962 V, respectively. In the measurement, the novel GMI sensor head was placed on the horizontal turntable in NMSS and the orientation change was performed by rotating the turntable by hand. The feedback voltage was picked up by the digital oscilloscope. The experimental results of a comparison between the feedback voltage of the developed circuit and the feedback voltage of the circuit without feedback were shown in Fig. 5. It is obvious that the feedback voltage fluctuation for the circuit without feedback is rather huge. By comparison, the feedback voltage for the developed circuit shows a negligible fluctuation, and its mean value is 0.958 V, equivalent to the bias magnetic field of 1 Oe according to the equation (5). The results reveal that the developed circuit can automatically adjust the bias magnetic field to keep it in its initial value no matter what the orientation is.

To validate the proposed method, the experiment on the output stability of the GMI sensor with the developed circuit was performed in NMSS. The GMI sensor with the developed circuit and the Helmholtz coil were placed on the turntable. Considering the DC magnetic field will be suppressed by the developed circuit, a AC magnetic field generated by supplying a sine waveform current to the Helmholtz coil was used as the detected signal. The frequency and amplitude of

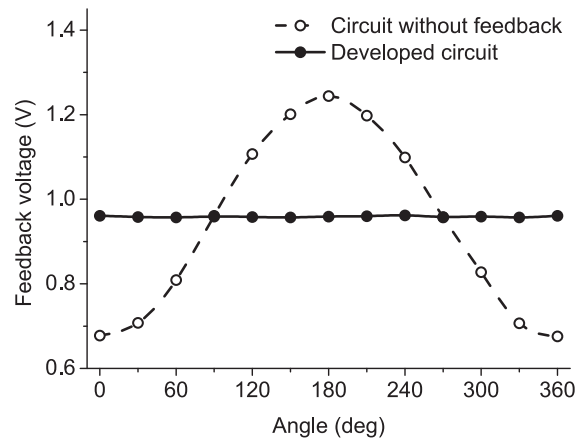


Fig. 5. Feedback voltage for the developed circuit and the circuit without feedback

the sinusoidal magnetic field were set to 10 Hz and 10 mOe, respectively. After adding the developed circuit, the gain of the sensor circuit was adjusted to obtain a high sensitivity. Fig. 6 illustrates the experimental result of the final output amplitude of the GMI sensor with the developed circuit versus the rotary angle. The final output voltage varies between 1.641 V and 1.651 V. The sensor circuit noise is responsible for the output fluctuation. Thus, it can be concluded that the orientation change had little effect on the output of the GMI sensor in NMSS.

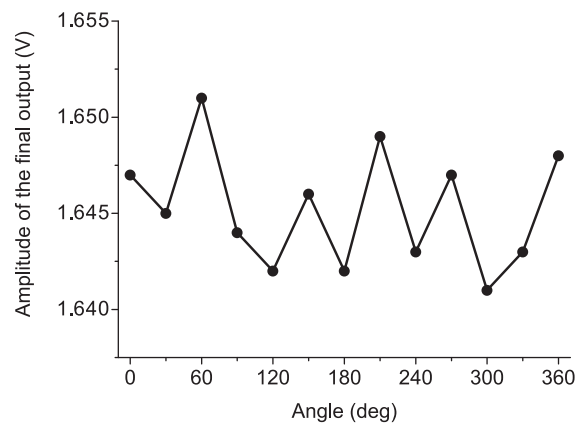


Fig. 6. Final output amplitude of the GMI sensor

Table I shows measured results of GMI sensor output amplitude for the method of keeping sensing direction perpendicular to the geomagnetic field (method A), the method of magnetic shielding (method B) and the proposed method. According to Table I, the output fluctuation of GMI sensor using the proposed method is close to ones using the other two methods. By comparison, the proposed method has advantages of high output stability and removing the limitation of sensing direction and magnetic shielding. Moreover, the use of the proposed method will increase the cost of sensor circuit compared with the other two methods.

Fig. 7 illustrates a photograph of the GMI sensor with the circuit implementing the proposed method.

Table I. Fluctuation comparison with previous methods

Method	0 (deg)	90 (deg)	180 (deg)	270 (deg)	360 (deg)
Method A	—	1.644 V	—	1.656 V	—
Method B	1.645 V	1.647 V	1.644 V	1.643 V	1.648 V
Proposed method	1.647 V	1.644 V	1.642 V	1.648 V	1.649 V

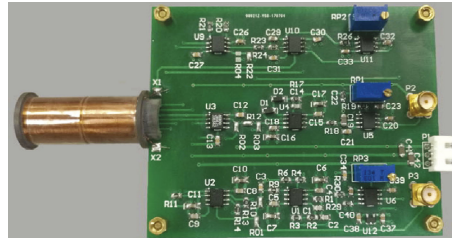


Fig. 7. Photograph of the GMI sensor with the developed circuit

5 Conclusion

The proposed method has effectively suppressed output instability of GMI sensors induced by the orientation without any magnetic shielding. The analog circuit that implements the proposed method is capable of automatically adjusting the bias magnetic field to make it always work in its initial value no matter what the orientation is. According to the principle of the developed circuit, the proposed approach can also get rid of the influence of the static ferromagnet around the GMI sensor on the sensor output. It should be pointed out that the addition of the circuit implementing the proposed method will lead to an increase in the cost and the power dissipation of the GMI sensor. However, the employment of the method gives the GMI sensor advantages for many engineering applications in the field of magnetic anomaly detection. For example, the GMI sensor with the developed circuit can be used in the mobile carriers such as vehicles, ships, airplanes and portable instruments for magnetic anomaly detection.

Acknowledgments

This work has been supported by the National Natural Science Foundation of China (No. 91320202).